



Full Length Article

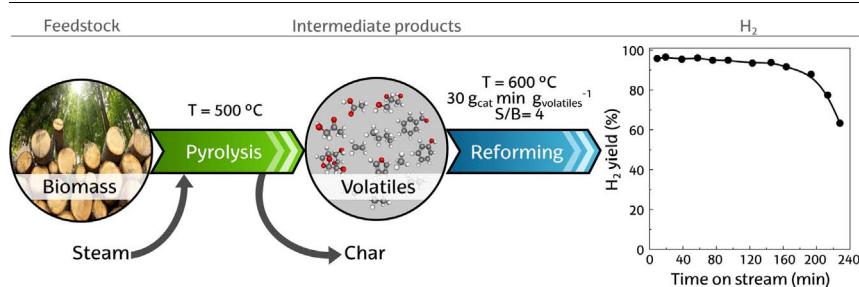
Role of operating conditions in the catalyst deactivation in the in-line steam reforming of volatiles from biomass fast pyrolysis



Aitor Arregi, Gartzzen Lopez*, Maider Amutio, Maite Artetxe, Itsaso Barbarias, Javier Bilbao, Martin Olazar

Department of Chemical Engineering, University of the Basque Country UPV/EHU, P.O. Box 644, E48080 Bilbao, Spain

GRAPHICAL ABSTRACT



ARTICLE INFO

Keywords:
Biomass
Pyrolysis
Reforming
Hydrogen
Deactivation
Bio-oil

ABSTRACT

The effect of reforming conditions (temperature, space time and steam/biomass ratio (S/B)) has been studied in the continuous biomass pyrolysis and in-line catalytic steam reforming process in order to establish suitable conditions for attenuating the deactivation of a commercial Ni catalyst by coke deposition. The experiments have been performed in a conical spouted bed and a fluidized bed reactor for the pyrolysis and reforming steps, respectively. Biomass fast pyrolysis was performed at 500 °C and the reforming operating conditions studied are as follows: 550–700 °C; space time, 10–30 g_{cat} min g_{volatiles}⁻¹, and; S/B ratio, 2–5. The coke deposited on the catalyst has been analyzed by temperature programmed oxidation (TPO), and two types of coke have been identified, i.e., the coke deposited on the Ni active sites and the one separated from these sites, without filamentous coke being observed by transmission electron microscopy (TEM). Coke deposition has been related to the decomposition of the oxygenates derived from biomass pyrolysis and the re-polymerization of phenolic oxygenates. Suitable conditions to achieve almost full conversion with a H₂ yield of up to 95% and stability for 160 min on stream, are as follows: 600 °C, space time of 30 g_{cat} min g_{volatiles}⁻¹ and S/B ratio of 3.

1. Introduction

Renewable fuels have attracted significant interest over the last years due to the environmental problems related to the massive use of petroleum based fuels, such as global warming and climate change [1]. In this scenario, biomass is considered one of the most important renewable raw materials with virtually no net contribution to global

greenhouse gas [2]. Thermochemical routes (such as gasification and fast pyrolysis) are regarded as the best strategies in terms of their scalability for conversion of biomass into bio-fuels [3]. High bio-oil yields can be obtained at moderate temperatures (around 500 °C) from different types of biomasses and in a delocalized way by using simple design fast pyrolysis technologies [4,5].

Amongst the different alternatives for bio-oil valorization, steam

* Corresponding author.

E-mail address: gartzzen.lopez@ehu.eus (G. Lopez).

reforming has received increasing attention for sustainable H₂ production [6–8]. The main interest of this process lies in its contribution to attenuating the current CO₂ emissions (produced from CH₄ reforming). Moreover, the bio-oil dehydration step, which is required for its valorization as fuel, is not needed for reforming. There are a considerable number of studies dealing with bio-oil reforming and the evolution of reaction indices with time on stream [9–11]. Remón et al. [8] studied the reforming of different bio-oils and reported full carbon conversion in the reforming of pine bio-oil at zero time on stream, and a decrease to 40% in 120 min on stream. The effect of temperature on conversion was also studied in the 500–800 °C range by Remiro et al. [12], who obtained full conversion for 5 h above 700 °C. Nevertheless, several challenges should be faced to avoid bio-oil handling problems in the reforming process [13,14]. Thus, in order to avoid these problems and those related to bio-oil storage, the capability of pyrolysis-reforming of biomass for H₂ production has been recently proven by several authors [15–18] by combining two in-line reactors for biomass fast pyrolysis and the subsequent reforming of volatiles, which allow obtaining a H₂-rich gaseous product.

In previous papers, the good behaviour of the pyrolysis-reforming process by means of a conical spouted bed reactor (CSBR) and an in-line fluidized bed reactor (FBR) has been verified for different feeds, such as biomass [17], high density polyethylene (HDPE) [19], polystyrene (PS) [20] and biomass/HDPE mixtures [21]. In these studies, the performance of the CSBR is proven for pyrolysis of irregular texture or/and sticky materials, specifically for biomass [22–24]. Besides, the FBR is a suitable reactor for reforming, as it allows attaining a homogeneous temperature and attenuating operational problems reported in the literature for fixed bed reactors due to the high amount of coke deposited on the catalyst [25].

Nevertheless, the deactivation of the catalyst is a determining factor for its selection, reactor design, establishment of the optimum operating strategy and viability of pyrolysis-reforming of biomass when scaling up. Although pyrolysis-reforming studies dealing with the characterization of deactivated catalysts are very scarce in the literature, it is well-established that coke deposition is the main deactivation cause of Ni based catalysts [26–29]. The deactivation rate is a consequence of coke formation and gasification rates, which are influenced by reaction conditions [12,30]. In order to improve catalyst activity and stability, different metal phases and promoters have been investigated in the reforming of bio-oil [31–33]. Rioche et al. [34] used a 1% Pt/CeZrO₂ catalyst and obtained low catalyst deactivation after 9 h on stream. Valle et al. [35] obtained higher stability of a Ni/ α -Al₂O₃ catalyst by adding La₂O₃ as promoter. Fu et al. [36] also reported higher stability of a Ni-Ce/Al₂O₃ catalyst up to 6 h on stream.

The aim of this study is to investigate the effect reforming temperature, space time and steam/biomass (S/B) ratio have on the reforming products, and especially on catalyst deactivation, with the objective of establishing suitable conditions for attenuating this problem. Accordingly, an original continuous two-step pyrolysis-reforming process has been developed, which is a novel alternative to the indirect bio-oil reforming strategy and avoids the operational problems related to bio-oil handling. In addition, the pyrolysis-reforming process allows for treating the whole biomass derived volatile stream, including bio-oil and gaseous products, which involves a remarkable advantage compared to the bio-oil reforming process. Thus, the mentioned different composition of the stream fed into the reforming step in the in-line pyrolysis-reforming strategy justifies a detailed investigation on the influence operating conditions have on catalyst deactivation, given that the results obtained for the steam reforming of bio-oil [9–12] are not applicable for this case. Moreover, coke content and type have been determined by temperature programmed oxidation (TPO) and transmission electron microscopy (TEM), in order to understand the role of coke in catalyst deactivation.

Table 1
Properties of the pine wood sawdust used in the study.

<i>Ultimate analysis (wt%)</i>	
Carbon	49.33
Hydrogen	6.06
Nitrogen	0.04
Oxygen	44.57
<i>Proximate analysis (wt%)</i>	
Volatile matter	73.4
Fixed carbon	16.7
Ash	0.5
Moisture	9.4
HHV (MJ kg ⁻¹)	19.8

2. Experimental

2.1. Materials

Table 1 shows the properties of the pine wood sawdust used in this study (particle size in the 1–2 mm range), which have been determined by ultimate and proximate analyses by means of a LECO CHNS-932 elemental analyzer and a TGA Q5000IR thermogravimetric analyzer, respectively. Moreover, a Parr 1356 isoperibolic bomb calorimeter has been used for the measurement of the higher heating value (HHV).

In addition, a commercial catalyst (G90-LDP) for CH₄ reforming has been used in the reforming step of biomass pyrolysis volatiles, which has been supplied by Süd Chemie (Germany) in the form of ribbed-rings having 10 hole ring shape and 19 × 16 mm size. Nevertheless, a particle size between 0.4 and 0.8 mm was required to attain a stable fluidization regime in the FBR, and therefore the catalyst had to be ground and sieved to that particle size. The chemical formulation of the catalyst is based on NiO (nominal content of 14 wt%), CaAl₂O₄ and Al₂O₃. The results obtained by N₂ adsorption-desorption technique (Micromeritics ASAP 2010) have been reported in previous studies [25,37] and revealed a low BET surface area of the catalyst (19 m² g⁻¹) and an average pore diameter of 122 Å.

Moreover, the catalyst has been reduced in-situ by feeding a 10 vol % H₂ at 710 °C for 4 h. The reduction temperature was determined by the results obtained in an AutoChem II 2920 Micromeritics by temperature programmed reduction (TPR), with the results being available in previous papers by the research group [25,37]. Two main peaks were observed at around 550 and 700 °C, which were related to the reduction of NiO and NiAl₂O₄ phases, respectively.

2.2. Reaction equipment

The bench scale laboratory plant used for pyrolysis-reforming of biomass is provided with the following elements: pyrolysis reactor (conical spouted bed reactor, CSBR) and catalytic reforming reactor (fluidized bed reactor, FBR). These devices together with all interconnection pipes are located inside a forced convection oven in order to maintain the box temperature at 300 °C and avoid the condensation of heavy compounds upstream and downstream the FBR, which in the latter case is essential to avoid the condensation of volatile products prior to their chromatographic analysis. The overall scheme of the plant is shown in Fig. 1.

The CSBR has been previously used by the research group in the pyrolysis and gasification of biomass [22,24,38], plastics [39–41] and tyres [42,43] and has been designed with the following dimensions: height of the conical section, 73 mm; diameter of the cylindrical section, 60.3 mm, angle of the conical section, 30°; diameter of the bed bottom, 12.5 mm, and; diameter of the gas inlet, 7.6 mm. Moreover, a gas preheater is located below the CSBR, which consists of a stainless steel cylindrical shell, with 310 mm in height and 27 mm in internal diameter. It is filled with stainless steel pipes that increase the surface area for heat transfer and heat the gases to the reaction temperature.

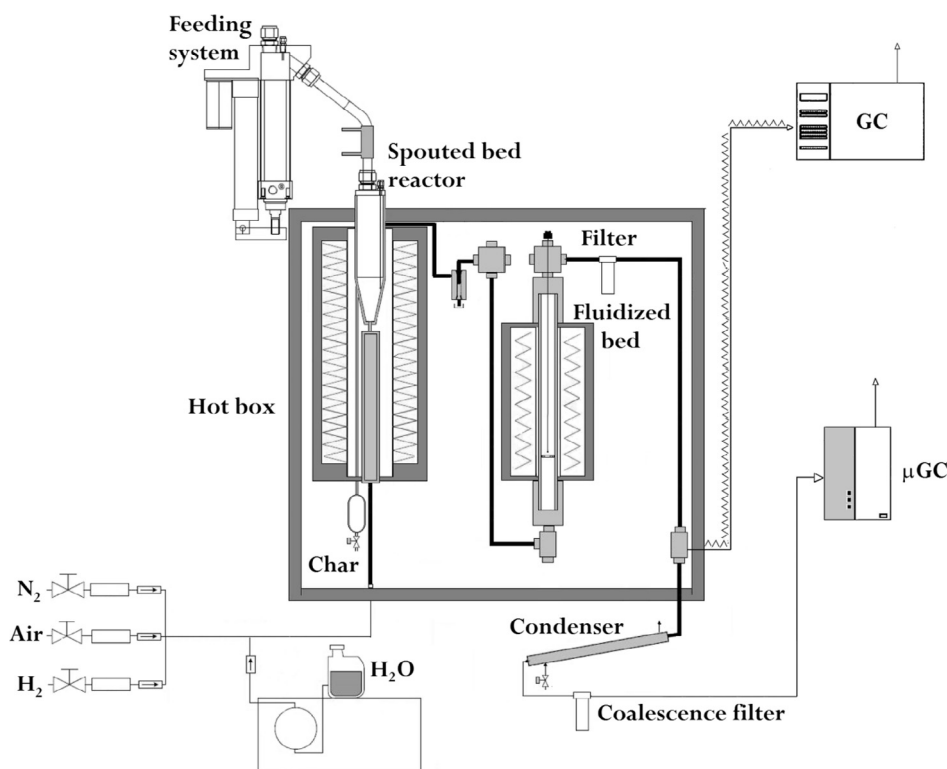


Fig. 1. Scheme of the laboratory scale pyrolysis-reforming plant.

Both the CSBR and gas preheater are located inside a 1250 W oven, which provides the heat required to reach the reaction temperature and preheat the gaseous stream to the reaction temperature. Moreover, the char formed is continuously removed from the pyrolysis reactor by means of a lateral outlet pipe to avoid its accumulation in the bed (see Fig. 1).

A FBR with a length of 440 mm and an internal diameter of 38.1 mm has been used for the in-line catalytic reforming of biomass pyrolysis volatiles. The reactor is located inside a 550 W oven, and provides the heat required to maintain the reaction temperature, which is controlled by a thermocouple inside the catalyst bed.

The biomass feeding system consists of a cylindrical vessel equipped with a vertical shaft connected to a piston placed below the biomass bed. While the piston rises, the whole system vibrates and the feeding is discharged through a pipe cooled with tap water. A *Gilson 307* pump has been used to supply the reactor with water, which is vaporized prior to entering the gas preheater in a heating cartridge located inside the hot box.

Moreover, the pilot plant is provided with a solid-gas separation system equipped with a cyclone and a filter, in order to remove the char and sand particles entrained from the pyrolysis reactor and the small particles of the catalyst entrained by attrition in the reforming reactor, respectively. In addition, the liquid-gas separation system is provided with a condenser and a coalescence filter.

2.3. Product analysis

The in-line analysis of the volatiles derived from the reforming reactor has been carried out by means of a GC Agilent 6890, which is equipped with a HP-Pona column and a flame ionization detector (FID). A sample of the reforming reactor outlet stream (prior to condensation) has been injected into the gas chromatograph by means of a line thermostated at 280 °C. On the other hand, the non-condensable gases (H_2 , CO_2 , CO , CH_4 and C_2 – C_4 hydrocarbons) have been analyzed in-line in a micro GC Varian 4900, once the outlet stream of the reforming reactor has been condensed and filtered.

The coke content deposited on the catalyst has been studied at the end of the continuous runs by temperature programmed oxidation (TPO) in a thermobalance connected to a *Balzers Instruments Thermostar* mass spectrometer. Given that the Ni on the catalyst is oxidized together with the carbonaceous coke, this procedure allows monitoring CO_2 formation throughout the TPO runs. The procedure used is as follows: (i) signal stabilization with a He stream ($10\text{ mL}\cdot\text{min}^{-1}$) at 100 °C, and (ii) oxidation with air ($50\text{ mL}\cdot\text{min}^{-1}$) following a ramp of $5\text{ }^\circ\text{C}\cdot\text{min}^{-1}$ to 800 °C, which has been kept for 30 min to guarantee total coke combustion. In addition, the nature of the coke deposited has been analyzed by transmission electron microscopy (TEM) images (Philips CM200).

2.4. Experimental conditions

In order to set suitable operating conditions in the pyrolysis step, the selected temperature has been 500 °C, given that below this temperature the biomass is not completely degraded and above this one the liquid fraction (bio-oil) decreases [44]. Moreover, the steam flow rate and particle size of the sand in the conical spouted bed reactor, and catalyst and sand particle sizes in the fluidized bed reactor, are conditioned by fluid dynamic requirements in both reactors in-line, given that the former is spouted and the latter fluidized with a common gas flow. Based on fluid dynamic runs in both reactors, a water flow rate of $3\text{ mL}\cdot\text{min}^{-1}$ has been established as suitable, which corresponds to a steam flow of $3.73\text{ NL}\cdot\text{min}^{-1}$, with 50 g of sand in the CSBR bed (particle size in the 0.3–0.35 mm range) for attaining a vigorous movement. In the FBR, the bed contains 25 g (mixture of catalyst and sand, with catalyst content being established by space time), with the particle size of the catalyst and the sand being in the 0.4–0.8 mm and 0.3–0.35 mm ranges, respectively. The fluidization velocity is between 3 and 4 times the minimum one, which ensures both stable fluidization of the bed, even when the catalyst has a high coke content, and moderate attrition of the catalyst.

In the steam reforming of biomass pyrolysis products, the effect of temperature has been studied at 550, 600, 650 and 700 °C, with a space

time of $20 \text{ g}_{\text{cat}} \text{ min g}_{\text{volatiles}}^{-1}$ and a S/B ratio of 4. It should be noted that a minimum reaction temperature of 550°C has been established, given that below this temperature the conversion of biomass pyrolysis volatiles is very low, which causes operational problems and high coke deposition on the catalyst. The ceiling reaction temperature is conditioned by the reduction temperature of the catalyst (710°C), so that higher temperatures lead to irreversible deactivation of the catalyst by Ni sintering. Similarly, the effect of space time has been studied between 10 and $30 \text{ g}_{\text{cat}} \text{ min g}_{\text{volatiles}}^{-1}$ at 600°C with a S/B ratio of 4. Finally, the effect of S/B ratio has been studied in the 2–5 range (S/C ratios in the 3.9–9.7 range), which has been attained by keeping the water flow rate at 3 mL min^{-1} and varying the amount of biomass fed into the process in the $0.6\text{--}1.5 \text{ g min}^{-1}$ range in order to ensure suitable fluid dynamic conditions and maintain the same space time value.

2.5. Reaction indices

The conversion was determined as a percentage of the C units contained in the volatiles fed into the reforming step that are recovered in the gaseous product (CO , CO_2 , CH_4 and $\text{C}_2\text{--C}_4$ hydrocarbons, mainly ethylene and ethane). The C content of the volatiles fed into the reforming reactor has been determined based on the composition of the pyrolysis outlet stream, so that the difference between the C content in the biomass and in the pyrolysis outlet stream is the C contained in the char, which is removed from the first reactor.

$$X(\%) = \frac{C_{\text{gas}}}{C_{\text{volatiles}}} 100 \quad (1)$$

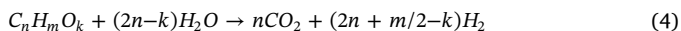
The yields of C containing products have been quantified based on the flow rate of C units in each product (F_i) and the flow rate of C units in the biomass pyrolysis volatile stream ($F_{\text{volatiles}}$) fed into the reforming reactor.

$$Y_i(\%) = \frac{F_i}{F_{\text{volatiles}}} 100 \quad (2)$$

In addition, H_2 yield is stated as a percentage of the maximum allowable by stoichiometry, considering all oxygenated compounds are converted into H_2 and CO_2 .

$$Y_{\text{H}_2}(\%) = \frac{F_{\text{H}_2}}{F_{\text{H}_2}^0} 100 \quad (3)$$

where F_{H_2} is the molar flow rate of H_2 produced in the reforming step and $F_{\text{H}_2}^0$ the maximum molar flow rate allowable by stoichiometry:



Finally, H_2 production is defined by mass unit of the biomass in the feed into the pyrolysis-reforming system, and has been calculated as follows:

$$P_{\text{H}_2}(\text{wt}\%) = \frac{m_{\text{H}_2}}{m_0} 100 \quad (5)$$

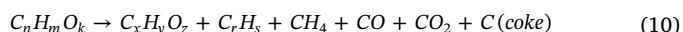
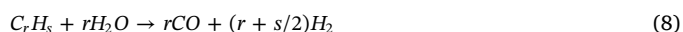
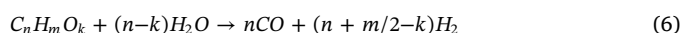
where m_{H_2} and m_0 are the mass flow rates of the H_2 produced and the biomass fed into the system, respectively.

3. Results

A study has been carried out on the effect reforming conditions (temperature, space time and S/B ratio) have on conversion, product yields and catalyst deactivation. All experiments have been performed using a pyrolysis temperature of 500°C , given that the production of oxygenated volatiles is maximized at this temperature in the CSBR [44]. A temperature between 500 and 600°C has also been used by other authors in the pyrolysis step, with pine wood in the feed [26,45–48]. Moreover, a comparison between biomass pyrolysis with N_2 and steam has been carried out in a previous paper, with the effect of the fluidizing agent (N_2 or steam) on product distribution being insignificant due to

the relatively low temperature (500°C) and short residence time of the volatiles in the CSBR [17]. Thus, 75 wt% of bio-oil, 8 wt% of gases and 17 wt% of char are obtained in the biomass pyrolysis in a CSBR. The bio-oil contains water (25 wt%) and a mixture of different oxygenated compounds, with the main products being phenols (16.5 wt%), ketones (6.4 wt%), saccharides (4.5 wt%), furans (3.3 wt%), acids (2.7 wt%), alcohols (2.0 wt%) and aldehydes (1.9 wt%). Moreover, the gas fraction is mainly made up of CO (3.4 wt%), CO_2 (3.3 wt%) and a low concentration of CH_4 (0.4 wt%), $\text{C}_2\text{--C}_4$ hydrocarbons (0.3 wt%) and H_2 (0.004 wt%). Consequently, the composition of the volatiles fed into the reforming step is the one corresponding to this stream and the reforming steam flow rate.

Furthermore, in order to explain the product distributions obtained, the following reactions have been considered in the reforming step: steam reforming of oxygenated compounds (Eq. (6)), CH_4 (Eq. (7)) and $\text{C}_2\text{--C}_4$ hydrocarbons (Eq. (8)), water gas shift (WGS) reaction (Eq. (9)) and decomposition/cracking of oxygenated compounds (Eq. (10)), with the latter being one of the reactions responsible for coke formation.



3.1. Effect of reforming temperature

The effect of temperature on catalyst deactivation has been studied between 550 and 700°C , and all the results have been obtained with a space time of $20 \text{ g}_{\text{cat}} \text{ min g}_{\text{volatiles}}^{-1}$ and a S/B ratio of 4. As observed in Fig. 2, at 550°C the conversion obtained at zero time on stream is low (< 60%), whereas above 600°C almost full conversion is achieved under these conditions, in which thermodynamic equilibrium is reached. A higher conversion was also obtained when temperature was increased in several studies dealing with pyrolysis-reforming of biomass [15,49–51], reforming of the bio-oil aqueous fraction [52–54] and reforming of raw bio-oil [36,55,56].

Concerning the evolution of conversion with time on stream, at 550°C it decreases from 58.3 to 36.9% in 20 min. However, between 600 and 700°C the decrease in conversion with time on stream is not very significant until 70–80 min on stream, and subsequently is very

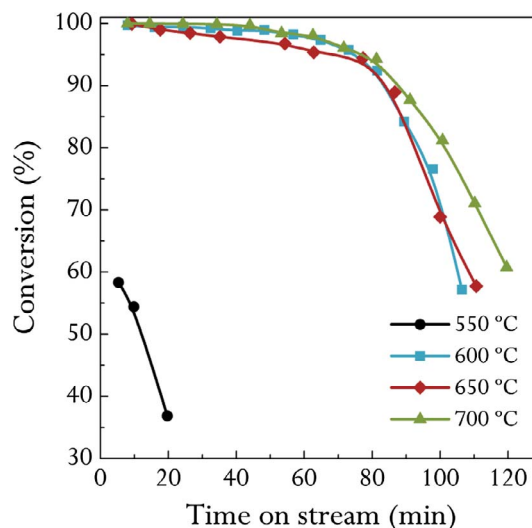


Fig. 2. Effect of reforming temperature on the evolution of conversion with time on stream. Reforming conditions: space time, $20 \text{ g}_{\text{cat}} \text{ min g}_{\text{volatiles}}^{-1}$; S/B ratio, 4.

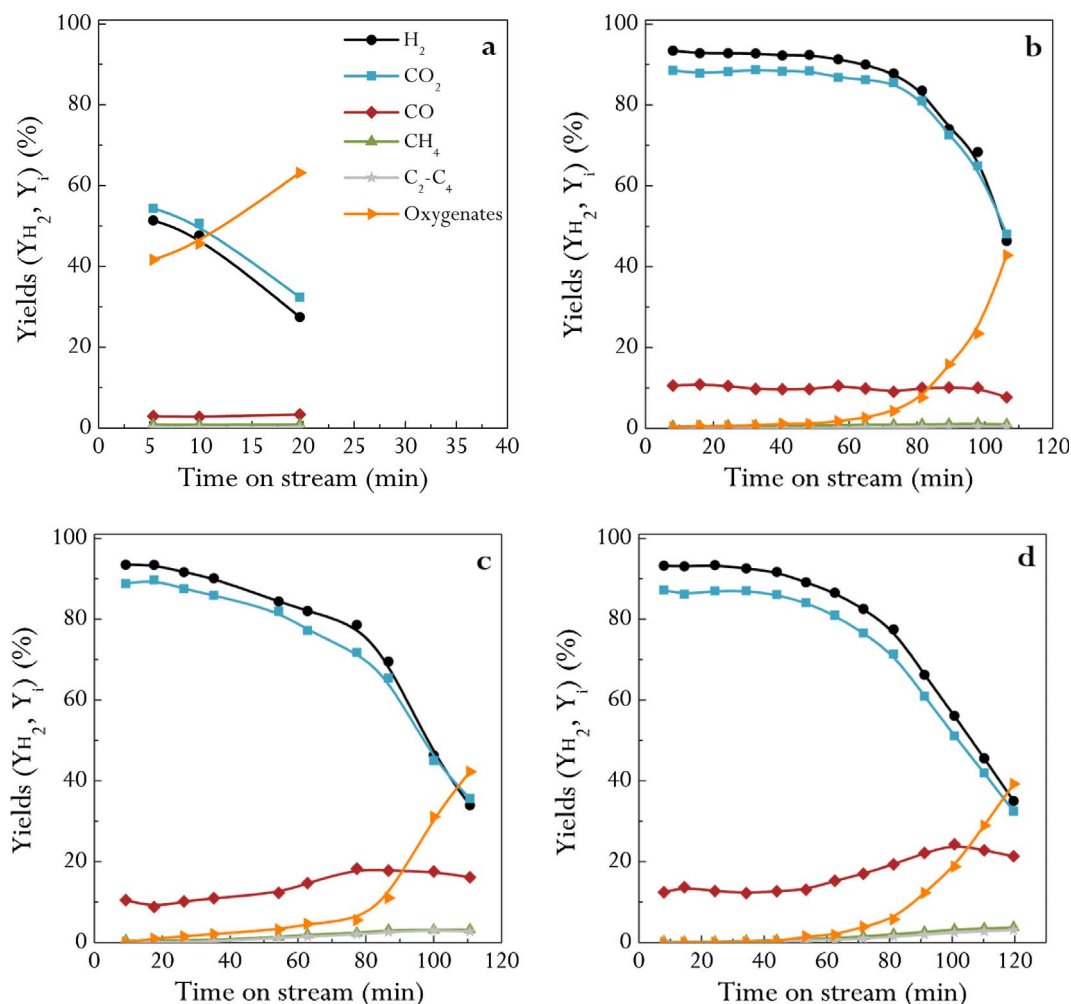
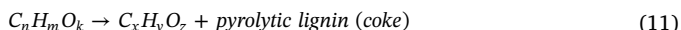


Fig. 3. Effect of reforming temperature on the evolution of product yields with time on stream at 550 °C (a), 600 °C (b), 650 °C (c) and 700 °C (d). Reforming conditions: space time, 20 $\text{g}_{\text{cat}} \text{min g}_{\text{volatiles}}^{-1}$; S/B ratio, 4.

pronounced, with this trend being slightly less pronounced at 700 °C. As observed, there is an acceleration of deactivation with time on stream once the catalyst starts deactivating and the concentration of non-reformed oxygenated compounds increases in the reaction medium. This trend is attributable to the role of these oxygenated compounds as coke precursors, which is well-established in the literature for bio-oil reforming [29,57]. These authors highlight the fact that coke formation takes place by decomposition of oxygenated compounds, Eq. (10), and re-polymerization of phenolic compounds derived from lignin pyrolysis:



Remiro et al. [12] attenuate the impact of this coke formation mechanism in the reforming of bio-oil by a controlled deposition of pyrolytic lignin, which reduces the concentration of phenolic compounds fed into the reforming reactor.

Fig. 3 shows the evolution of the yields of H_2 , CO_2 , CO , CH_4 , $\text{C}_2\text{-C}_4$ hydrocarbons (mainly ethylene, ethane, propylene and propane) and oxygenated compounds (non-converted fraction) with time on stream, at 550 (a), 600 (b), 650 (c) and 700 °C (d). Initial H_2 yield increases from 54.4% at 550 °C to around 93.5% in the 600–700 °C range, which corresponds to an increase in H_2 production from 6.4 to around 11.0 wt %. Higher initial H_2 yields and productions are also obtained by several authors as reforming temperature is increased in the pyrolysis and in-line reforming of biomass in other reactors [15,46], which is due to the higher extent of the reforming reaction. Similarly, studies dealing with bio-oil reforming confirm a similar trend for H_2 yield

[36,52,53,55,56,58].

Moreover, it should be pointed out that H_2 yield decreases with time on stream due to catalyst deactivation with the same trend shown in Fig. 2 for conversion, with the initial decrease being more pronounced at 550 °C (Fig. 3a), from 51.4 at zero time on stream to 27.5% in 20 min, due to the increase in oxygenate concentration in the reaction medium. At 600 °C, and higher temperatures, the decrease in H_2 yield is only significant after a certain value of time on stream, which is caused by the autocatalytic effect of catalyst deactivation mentioned above due to the increase in the concentration of non-reformed oxygenates in the reaction medium. Accordingly, at 600 °C H_2 yield decreases slowly from 93.5 at zero time on stream to 87.8% in 75 min, with the decrease being subsequently more pronounced down to 46.4% in a period of 30 min approximately. H_2 yield follows a similar trend at 650 and 700 °C, although the decrease is more pronounced than that observed at 600 °C for the first 75 min, i.e., decreases from 93.5 to 78.6% in 77 min at 650 °C and from 93.2 to 82.5% in 72 min at 700 °C. Furthermore, CO_2 yield follows a similar trend as H_2 yield with time on stream, obtaining a similar value at all temperatures when the catalyst is deactivated. Regarding CO yield, it is maintained almost constant at 550 (~3%) and 600 °C (~10%), whereas it increases slightly with time on stream from 10.5 to 16.2% in 110 min at 650 °C and from 12.5 to 21.4% in 120 min at 700 °C. This effect of temperature on CO yield is attributable to the higher oxygenate decomposition rate, Eq. (10), and the displacement of the thermodynamic equilibrium of WGS reaction when temperature is increased. The increase in CO yield with time on stream is also a

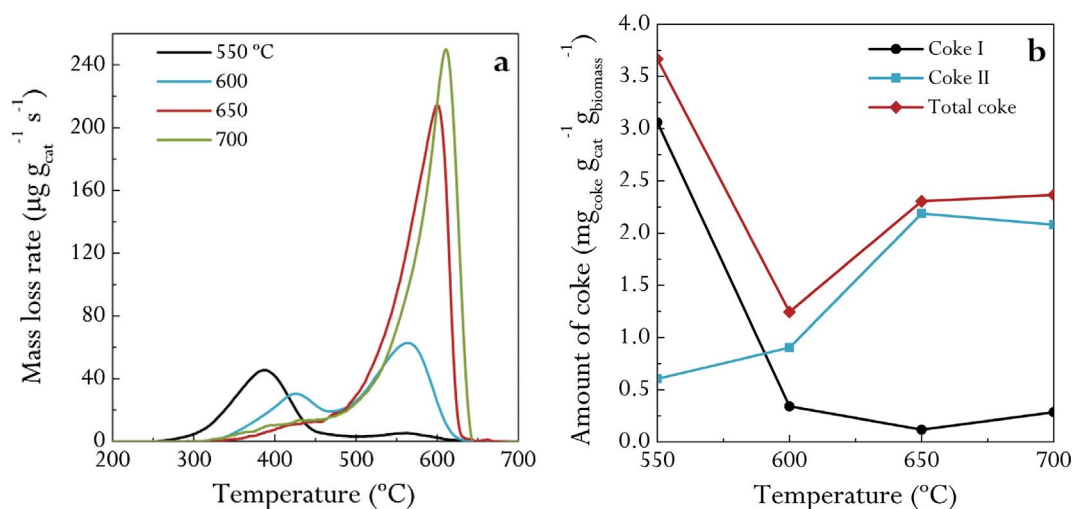


Fig. 4. Effect of reforming temperature on the TPO profiles of the deactivated catalyst (a) and total amount of coke deposited per biomass mass unit (b). Reforming conditions: space time, $20 \text{ g}_{\text{cat}} \text{ min g}_{\text{volatiles}}^{-1}$; S/B ratio, 4.

consequence of favouring the reaction of oxygenate decomposition (Eq. (10)) due to the higher concentration of these compounds in the reaction medium, given that the catalyst is deactivated for reforming reactions. Catalyst deactivation for WGS reaction can also contribute to these results.

In the 600–700 °C range (Fig. 3b–d), and as a consequence of the decrease in catalyst activity for the reforming reactions, the yields of CH₄, C₂–C₄ hydrocarbons (overlapped results) and non-converted oxygenates increase with time on stream in the whole temperature range studied, with the increase being exponential as catalyst deactivation is more severe. This trend is explained by thermal cracking reactions of oxygenated compounds to form CH₄ and C₂–C₄ hydrocarbons, Eq. (10), which occurs in parallel with the reforming reactions. Consequently, as the rate of the reforming reactions decreases due to catalyst deactivation, the formation of products by thermal cracking reactions is favoured.

In order to explain the effect temperature has on catalyst deactivation, the coke deposited at different temperatures has been analyzed by temperature programmed oxidation (TPO) and transmission electron microscopy (TEM) techniques. Thus, Fig. 4 displays the TPO profiles of the deactivated catalyst (Fig. 4a) and the amount of coke deposited (Fig. 4b) at the reforming temperatures studied. Considering the different peaks observed in the TPO profile (Fig. 4a), two different types of cokes may be distinguished, which are burnt at different temperatures. These different types of cokes have also been identified in deactivated Ni-based catalysts in the reforming of CH₄ [59,60], hydrocarbons [19,61–63] and oxygenated compounds, such as ethanol [64–69]. In these works, the coke that burns at low temperatures (< 450 °C) (coke I) is defined as amorphous coke and encapsulates Ni metallic sites (which promote its combustion), whereas the coke burning at higher temperatures (coke II) is separated from Ni active sites, more structured and evolves towards higher graphitization structures, even forming filamentous coke and carbon nanotubes (less common in the reforming of oxygenates and bio-oil).

As shown in Fig. 4a, an increase in reforming temperature causes the displacement of the peaks corresponding to the different types of cokes towards higher combustion temperatures. In the case of the amorphous coke, there is a pronounced displacement of its combustion peak as reforming temperature is increased from 550 to 600 °C, with the tops of the peaks being placed at around 380 and 425 °C, respectively. In the case of the structured coke, the effect of reforming temperature on peak position is less significant, with the top being placed at around 550, 560, 610 and 620 °C for the reforming temperatures of 550, 600, 650 and 700 °C, respectively. This displacement is explained by the

evolution of the coke to more condensed structures when reforming temperature is increased [70], making more difficult its combustion due to the less hydrogenated nature of the coke and its location in the catalyst particle farther from Ni sites.

Moreover, Fig. 4b shows the effect temperature has on the amount of the different types of cokes. It should be pointed out that the amount of coke has been given per mass unit of biomass fed into the system, given that reaction time is different in each experiment, as they were stopped when the catalyst was deactivated. Consequently, the values in Fig. 4b are the average rates of coke deposition. Table 2 shows the values of coke content (C_C), the reaction time, the biomass fed into the system and the amount of coke deposited per biomass mass unit (C_C′).

As observed in Fig. 4b, the amount of coke deposited per biomass mass unit on Ni active sites (coke I) decreases considerably when temperature is increased from 550 °C to 600 °C, with the decrease being less pronounced at higher temperatures. On the contrary, the amount of coke separated from Ni sites (coke II) increases steadily when temperature is increased, especially in the 600–650 °C range. As a consequence of the different trend of the two types of cokes, the amount of coke per biomass mass unit has a minimum value at 600 °C and increases from 1.25 to 2.37 mg_{coke} g_{cat}⁻¹ g_{biomass}⁻¹ in the 600–700 °C range. Wang et al. [71] also observed that the total amount of coke deposited on the catalyst was higher when temperature was increased.

Comparing the results in Fig. 4b with those corresponding to the evolution with time on stream in Figs. 2 and 3, catalyst deactivation is not directly related to coke content, but coke nature and location influences this deactivation, which in turn is related to the reaction conditions, with temperature and oxygenate concentration being of high significance. Thus, amorphous coke deposition is very high at 550 °C due to the significance of oxygenate decomposition and polymerization reactions, Eqs. (10) and (11), respectively, given that oxygenate concentration in the reaction medium is high at this

Table 2

Total coke content in the catalyst (C_C) and the total amount of coke deposited per biomass mass unit (C_C′) at different reforming temperatures. Reforming conditions: space time, $20 \text{ g}_{\text{cat}} \text{ min g}_{\text{volatiles}}^{-1}$; S/B ratio, 4.

Temperature (°C)	C _C (wt%)	Time on stream (min)	Biomass feed (g)	C _C ′ (mg _{coke} g _{cat} ⁻¹ g _{biomass} ⁻¹)
550	5.5	20	15	3.67
600	9.9	106	80	1.25
650	19.2	111	83	2.31
700	21.3	120	90	2.37

temperature. It is well-established in the literature [54,63,72,73] that amorphous coke is the main responsible for catalyst deactivation because it encapsulates Ni sites. Above 600 °C, oxygenate reforming reactions are favoured rather than thermal reactions, and presumably the gasification of the amorphous coke is also enhanced because it is located close to Ni particles. Moreover, oxygenate concentration in the reaction medium is lower when temperature is increased, and therefore their decomposition and polymerization reaction rates undergo attenuation. On the contrary, the amount of coke II (which is burnt at higher temperatures) deposited on the catalyst per biomass mass unit increases when reforming temperature is increased (Fig. 4b), attaining its maximum content at 700 °C. This trend at high temperatures is explained by the evolution of amorphous coke towards more refractory structures with lower capacity for Ni site blockage and gasification [69,70]. The high temperature needed for its combustion by TPO in Fig. 4a (620 °C for a reforming temperature of 700 °C) reveals the graphitic nature of coke II at this temperature. Moreover, the effect temperature has on the content of each type of coke cannot be clearly ascertained due to the different duration of the reactions. Thus, the duration of the reaction at 550 °C is short, and therefore the coke does not evolve towards more condensed structures. Furthermore, the contribution of Boudouard (Eq. (12)) and CH₄ decomposition (Eq. (13)) reactions to the formation of coke II cannot be excluded at high temperatures.



Fig. 5 shows the images of transmission electron microscopy (TEM) of the catalyst deactivated at 600 °C (Fig. 5a) and 700 °C (Fig. 5b), in which Ni particles are identified as dark areas. As observed, all Ni particles are coated with coke, whose structure is more ordered when temperature is increased.

Filamentous coke is not observed in Fig. 5, which is because the coke has a more disordered structure than in the reforming of other oxygenated compounds, such as ethanol [64,65,68] and, particularly, in the reforming of hydrocarbons [19,61,62]. Concerning biomass valorisation, the research group headed by Prof. Williams studied Ni-based deactivated catalysts in the pyrolysis and in-line reforming of biomass in batch regime, verifying that the composition of biomass pyrolysis products (with high content of phenols and water) is not suitable for the production of nano-structured materials and coke nature depends on the catalyst. Accordingly, Efika et al. [26] verified by SEM images the presence of filamentous carbon in a Ni/Al₂O₃ catalyst,

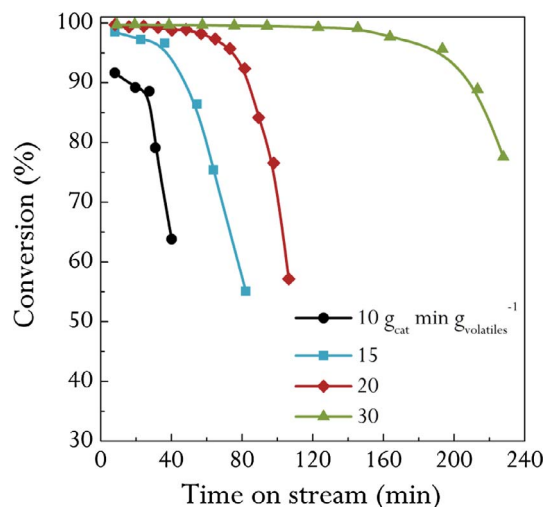


Fig. 6. Effect of reforming space time on the evolution of conversion with time on stream. Reforming conditions: 600 °C; S/B ratio, 4.

whereas carbon filaments are not clearly observed in a Ni/CeO₂/Al₂O₃ catalyst. Nahil et al. [27] observed two different carbon oxidation peaks in their TPO curve, one at around 450 °C (amorphous coke) and the other one at around 550 °C (filamentous coke). However, when rice husk, sugar cane bagasse and wheat straw were used as feedstock, the second peak was obtained at around 650 °C, which was assigned to graphitic carbon [28].

3.2. Effect of reforming space time

According to the results aforementioned in Section 3.1, 600 °C is the suitable temperature for attenuating catalyst deactivation and higher temperatures are not interesting due to the higher energy costs involved. Accordingly, the effect space time has on deactivation has been studied based on runs at 600 °C with a S/B ratio of 4 and space times of 10, 15, 20 and 30 g_{cat} min g_{volatiles}⁻¹. Fig. 6 shows the effect space time has on the evolution of conversion of pyrolysis volatiles with time on stream. As observed, when space time is increased a higher initial conversion is obtained, which has also been reported in several biomass pyrolysis-reforming studies [74,75]. Thus, an initial conversion higher than 98.5% is obtained above 15 g_{cat} min g_{volatiles}⁻¹, with the maximum conversion (and tar-free gas) being obtained with 20 g_{cat} min g_{volatiles}⁻¹.

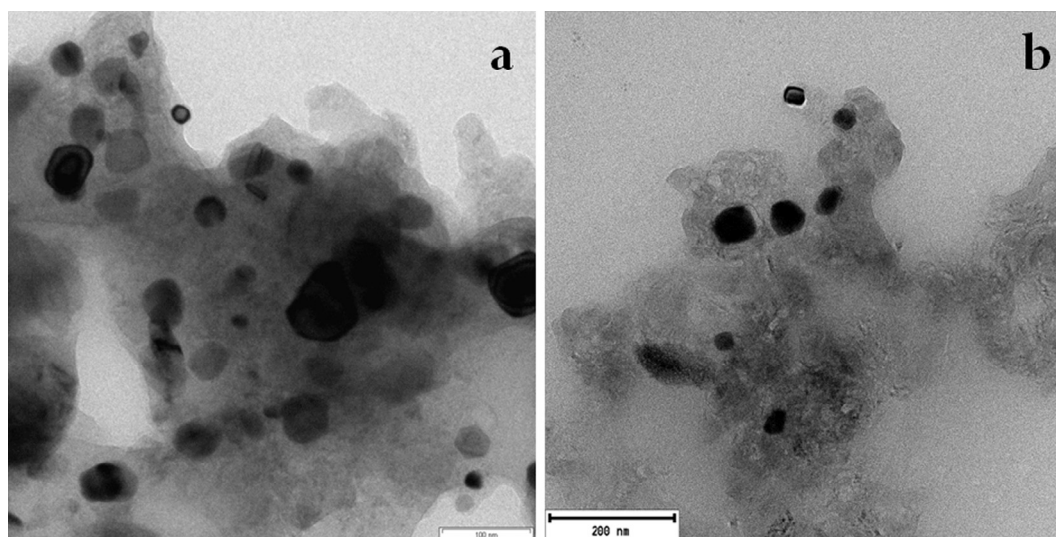


Fig. 5. TEM images of the catalyst deactivated at 600 °C (a) and 700 °C (b). Operating conditions: space time, 20 g_{cat} min g_{volatiles}⁻¹; S/B ratio, 4.

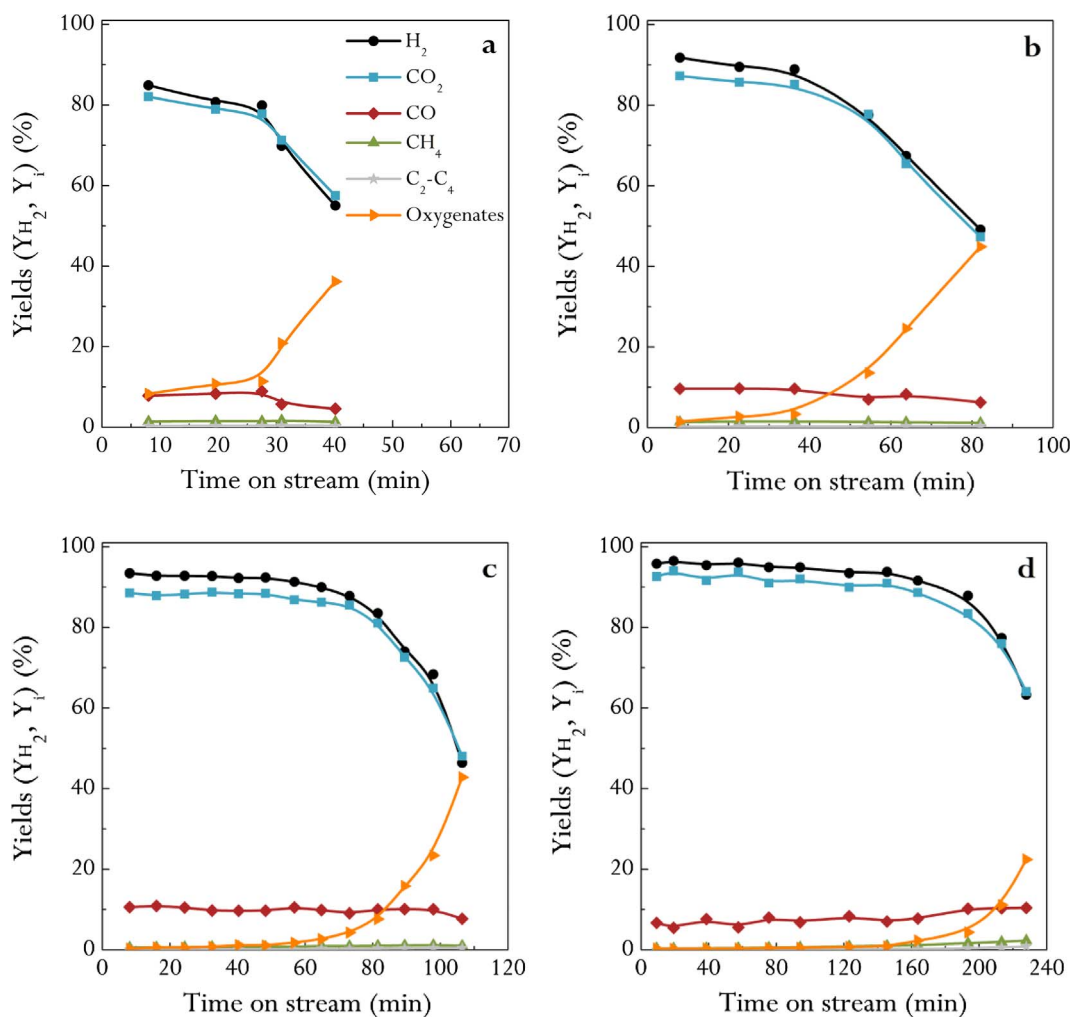


Fig. 7. Effect of reforming space time on the evolution of product yields with time on stream when using 10 (a), 15 (b), 20 (c) and 30 $g_{cat} \min g_{volatiles}^{-1}$ (d). Reforming conditions: 600 °C; S/B ratio, 4.

Concerning the evolution of conversion with time on stream (Fig. 6), catalyst deactivation is attenuated when space time is increased, which is explained by the role played by the non-converted oxygenated compounds as coke precursors. A higher lifespan of the catalyst at high space times is obtained in the reforming of bio-oil [12,76]. Therefore, almost full conversion is achieved in the first 160 min when a space time of 30 $g_{cat} \min g_{volatiles}^{-1}$ is used, whereas catalyst deactivation is significant for times on stream longer than 60 min when using 20 $g_{cat} \min g_{volatiles}^{-1}$, with the decrease in activity being pronounced subsequent to 75 min. Furthermore, when a space time lower than 15 $g_{cat} \min g_{volatiles}^{-1}$ is used, the decrease in conversion is significant after 20 min on stream.

Fig. 7 shows the effect space time has on the evolution of product yields with time on stream. When space time is increased, higher H_2 yields are obtained at zero time on stream due to the higher extent of reforming and WGS reactions, which is consistent with the literature on the reforming of bio-oil [6,36,77,78]. Moreover, the effect space time has on the initial CO and CO_2 yields is noteworthy. As observed, when space time is increased from 10 to 20 $g_{cat} \min g_{volatiles}^{-1}$ (Fig. 7a and c, respectively) the initial CO yield increases from 7.9 to 10.6% and the initial CO_2 yield from 82.1 to 88.6%. However, the initial CO yield decreases to 6.7% and that of CO_2 increases to 92.6% at the highest space time studied (Fig. 7d), with the yields of CH_4 and C_2-C_4 hydrocarbons being lower. This trend for CO and CO_2 yields when space time is increased is also reported in the literature for bio-oil reforming [13,52,79] and is evidence that both reforming and WGS reactions are

favoured at low space time values, whereas the WGS reaction is more favoured than reforming reactions at high space time values.

Concerning the evolution with time on stream of the product yields shown in Fig. 7, the decrease in H_2 yield is lower at high space time values, i.e., from 84.9 to 55.0% in 40 min with 10 $g_{cat} \min g_{volatiles}^{-1}$ and from 95.8 to 63.3% in 230 min with 30 $g_{cat} \min g_{volatiles}^{-1}$. Furthermore, the effect space time has on the decrease of CO_2 yield follows a similar trend, whereas CO yield does not follow a clear trend, with its value being between 6 and 10%. The slight effect of space time is evidence that the decrease expected in the reforming rate due to catalyst deactivation is compensated with the higher formation of CO by cracking of oxygenates, whose concentration is higher as the catalyst is being deactivated. In addition, the presence of CO is also favoured by catalyst deactivation for WGS reaction. However, the decrease in the rate of reforming reactions is also evident, i.e., the yields of CH_4 and C_2-C_4 hydrocarbons increase exponentially when time on stream increases (overlapped results), which is explained by the increase in the yield of non-converted oxygenates in the reaction environment. Therefore, cracking reactions are favoured, enhancing the formation of CH_4 and C_2-C_4 hydrocarbons [12,53,79,80].

Fig. 8a displays the TPO results obtained in the experiments carried out using different space times. Moreover, Fig. 8b and Table 3 show the coke contents of the deactivated catalyst. As aforementioned, the fact of using different catalyst masses and times on stream in each experiment (Table 3) has to be considered when comparing the results in Fig. 8b, in which the coke contents deposited per biomass mass unit fed into the

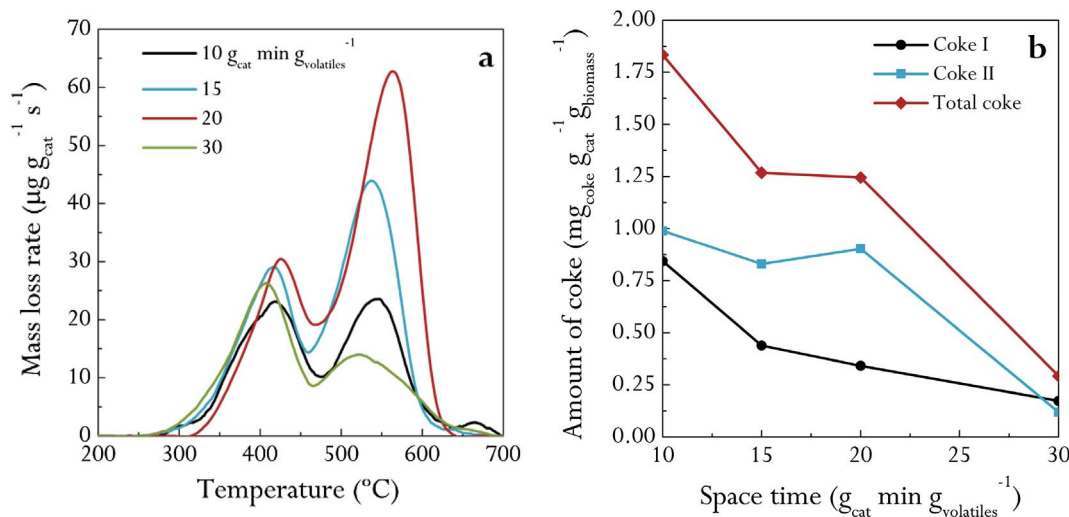


Fig. 8. Effect of space time on the TPO profiles of the deactivated catalyst (a) and total amount of coke deposited per biomass mass unit (b). Reforming conditions: 600 $^{\circ}\text{C}$; S/B ratio, 4.

Table 3

Total coke content in the catalyst (C_c) and the total amount of coke deposited per biomass mass unit (C_c') at different space times. Reforming conditions: 600 $^{\circ}\text{C}$; S/B ratio, 4.

Space time ($\text{g}_{\text{cat}} \text{min g}_{\text{volatiles}}^{-1}$)	C_c (wt%)	Time on stream (min)	Biomass feed (g)	C_c' ($\text{mg}_{\text{coke}} \text{g}_{\text{cat}}^{-1}$ $\text{g}_{\text{biomass}}^{-1}$)
10	5.5	40	30	1.83
15	7.8	82	62	1.27
20	9.9	106	80	1.25
30	5.0	228	171	0.29

system are shown. As observed, the total amount of coke per biomass mass unit decreases from 1.83 to 0.29 $\text{mg}_{\text{coke}} \text{g}_{\text{cat}}^{-1} \text{g}_{\text{biomass}}^{-1}$ when space time is increased in the 10–30 $\text{g}_{\text{cat}} \text{min g}_{\text{volatiles}}^{-1}$ range, given that a higher amount of catalyst enhances reforming reactions and reduces oxygenate concentration, which are the main coke precursors.

Considering the effect space time has on the amount of each type of coke deposited on the catalyst, it can be observed in Fig. 8b that the amount of coke I (which is burnt at low temperatures) per biomass mass unit decreases from 0.84 to 0.17 $\text{mg}_{\text{coke}} \text{g}_{\text{cat}}^{-1} \text{g}_{\text{biomass}}^{-1}$ as space time is increased in the 10–30 $\text{g}_{\text{cat}} \text{min g}_{\text{volatiles}}^{-1}$ range. This result can be explained by the thermal origin of this coke, which is produced by decomposition of oxygenates (Eq. (10)) and re-polymerization of phenolic compounds on the catalyst surface (Eq. (11)). Consequently, the progress of these reactions is disfavoured by the higher extent of oxygenate reforming and WGS reactions, as observed in the reforming of bio-oil [6,12,29]. However, when space time is increased in the 10–20 $\text{g}_{\text{cat}} \text{min g}_{\text{volatiles}}^{-1}$ range, the amount of coke II deposited per biomass mass unit remains constant, given that presumably this coke is formed mainly by evolution of the coke I towards more ordered structures, which depends on the different composition of the reaction environment and the times on stream for the different space time values. Moreover, a displacement of this coke peak is observed when space time is increased in Fig. 8a. This effect is a consequence of the higher duration of the reactions, and therefore a subsequent evolution of the coke to a more condensed structure. Nevertheless, this effect avoids the formation of coke II, which decreases when a space time of 30 $\text{g}_{\text{cat}} \text{min g}_{\text{volatiles}}^{-1}$ is used, due to the lower concentration of oxygenated compounds in the reaction environment. These conditions, in which a high space time value is used, are interesting from an industrial point of view, as the deposition of coke is limited. Thus, when a space time of 30 $\text{g}_{\text{cat}} \text{min g}_{\text{volatiles}}^{-1}$ is used, a maximum H_2 production of 11.7 wt% is obtained, with the catalyst being stable for more than 2 h.

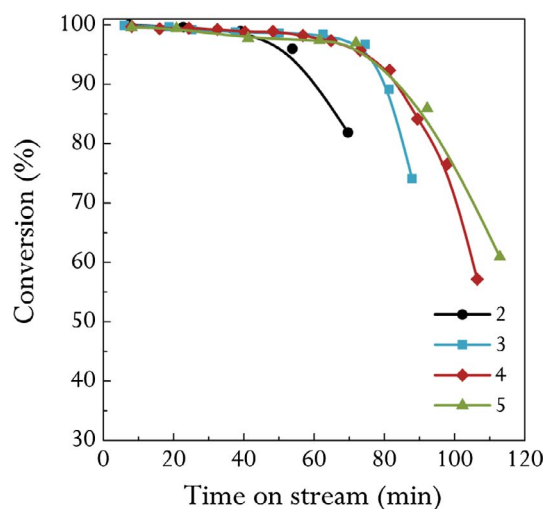


Fig. 9. Effect of S/B ratio on the evolution of conversion with time on stream. Reforming conditions: 600 $^{\circ}\text{C}$; space time, 20 $\text{g}_{\text{cat}} \text{min g}_{\text{volatiles}}^{-1}$.

3.3. Effect of S/B ratio

Fig. 9 shows the evolution of conversion with time on stream using different S/B ratios. The results correspond to S/B ratios of 2, 3, 4 and 5 (S/C ratios of 3.9, 5.8, 7.7 and 9.7, respectively), at 600 $^{\circ}\text{C}$ and a space time of 20 $\text{g}_{\text{cat}} \text{min g}_{\text{volatiles}}^{-1}$. As observed, the conversion at zero time on stream increases slightly from 99.5 to 100% when a high space time value is used and S/B ratio is increased from 2 to 5. However, the deactivation is attenuated considerably, in particular when S/B ratio is increased from 2 to 3. These results are explained by the lower concentration of oxygenated compounds (which are coke precursors) and the higher reforming rate of these oxygenates and intermediate compounds. However, above a S/B ratio of 4, its influence on conversion decrease is lower, which is attributable to the partial saturation of Ni active sites with adsorbed steam [81].

Fig. 10 shows the effect of S/B ratio on the evolution of product yields with time on stream. Most authors reported that a higher initial H_2 yield is obtained when S/B ratio is increased in the reforming of bio-oil [31,36,56,73]. In this study, the initial H_2 yield increases from 89.2 to 94.2% when S/B ratio is increased in the 2–5 range, due to the enhancement of reforming and WGS reactions, with CO_2 yield being higher and CO yield lower.

As mentioned above for conversion, the effect on catalyst deactivation is not so significant at high S/B ratios. Moreover, it should be

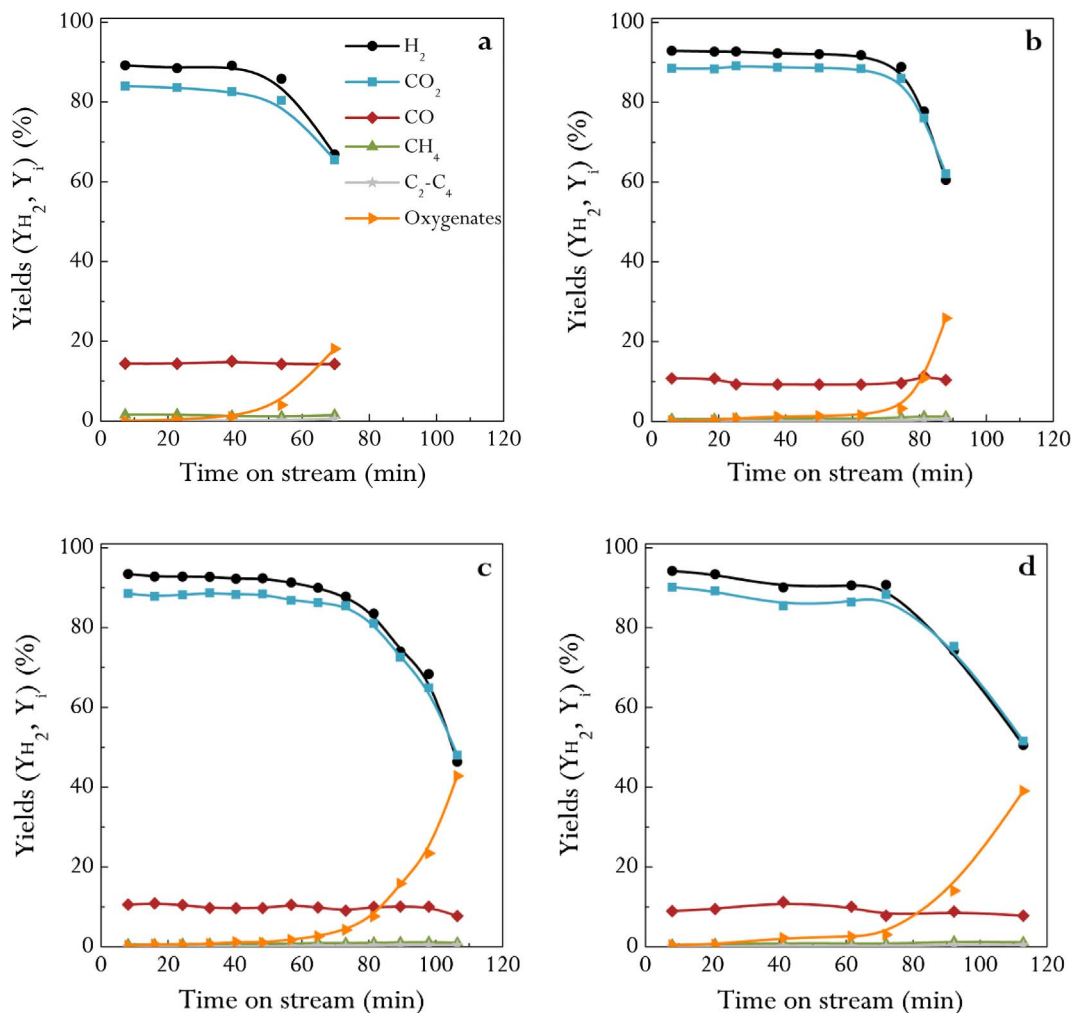


Fig. 10. Effect of S/B ratio on the evolution of product yields with time on stream with S/B ratios of 2 (a), 3 (b), 4 (c) and 5 (d). Reforming conditions: 600 °C; space time, 20 g_{cat} min g_{volatiles}⁻¹.

noted that the yields of CH₄ and C₂-C₄ hydrocarbons (produced by oxygenate decomposition reactions) and the presence of oxygenated compounds in the reaction environment is delayed when high S/B ratios are used, which has also been reported in studies dealing with the reforming of bio-oil [6,31,58,77]. The aforementioned results reveal

the interest of using an S/B ratio of 3, with H₂ yield being constant (around 93%) for 70 min under the conditions studied. A higher S/B ratio only improves slightly the deactivation results and has as counterpart higher energy requirements for water vaporization.

Fig. 11a displays the TPO profiles for the catalyst deactivated at

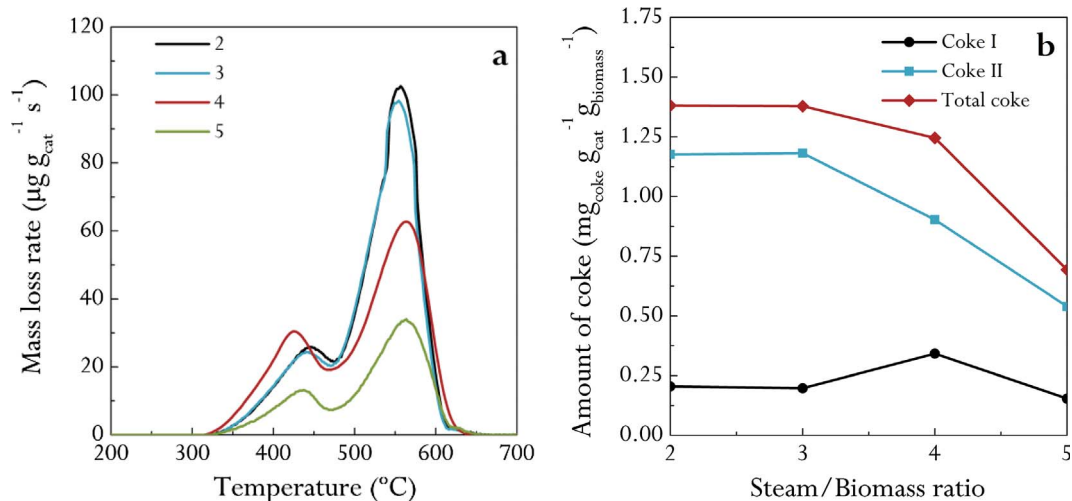


Fig. 11. Effect of S/B ratio on the TPO profiles of the deactivated catalyst (a) and total amount of coke deposited per biomass mass unit (b). Reforming conditions: 600 °C, space time, 20 g_{cat} min g_{volatiles}⁻¹.

Table 4

Total coke content in the catalyst (C_c) and total amount of coke deposited per biomass mass unit (C'_c) at different S/B ratios. Reforming conditions: 600 °C; space time, 20 $\text{g}_{\text{cat}} \text{min g}_{\text{volatiles}}^{-1}$.

S/B ratio	C_c (wt%)	Time on stream (min)	Biomass feed (g)	C'_c ($\text{mg}_{\text{coke}} \text{g}_{\text{cat}}^{-1} \text{g}_{\text{biomass}}^{-1}$)
2	14.5	70	105	1.38
3	11.3	82	82	1.38
4	9.9	106	80	1.25
5	4.7	113	68	0.69

different S/B ratios and Fig. 11b and Table 4 show the effect S/B ratio has on the amount of each type of coke deposited on the catalyst. Thus, the amount of coke deposited per biomass mass unit decreases from 1.38 to 0.69 $\text{mg}_{\text{coke}} \text{g}_{\text{cat}}^{-1} \text{g}_{\text{biomass}}^{-1}$ when S/B ratio is increased from 2 to 5, which has also been verified in the reforming of bio-oil [36,71,76]. Nevertheless, the effect S/B ratio has on the formation of each type of coke is different. The amount of coke I is almost constant when S/B ratio is increased, which is evidence that the formation of amorphous coke (through the reactions in Eqs. (10) and (11)) only depends on temperature and space time. However, the formation of coke II is disfavoured when S/B ratio is increased, given that the condensation of coke I components is attenuated. The fact that catalyst deactivation is lower when S/B ratio is increased (Figs. 9 and 10), with the amount of coke I being similar, is evidence that an increase in steam concentration is not effective for attenuating amorphous coke deposition, but avoids the isolation of Ni active sites, and therefore the effective deactivation is attenuated.

4. Conclusions

The good performance of a two in-line reactor system (CSBR-FBR) for biomass pyrolysis-reforming has been proven in a wide range of operating conditions. Nevertheless, the catalyst undergoes a severe deactivation with time on stream related to coke deposition, whose formation is attributable to the decomposition of oxygenated compounds and the re-polymerization of phenolic oxygenates. The TPO analysis of the coke allows identifying two different fractions, corresponding to the coke deposited on Ni active sites and the coke separated from these sites. Coke deposition and the resulting deactivation can be attenuated by selecting operating conditions in which the reforming and WGS reactions are favoured, and therefore the concentration of oxygenates (coke precursors) in the reaction medium is minimized. In order to achieve these objectives, a temperature of 600 °C and a S/B ratio of 3 have been chosen as suitable conditions. Moreover, catalyst stability is favoured when space time is increased, and a H_2 yield of 95.8% is achieved for 160 min on stream for a space time of 30 $\text{g}_{\text{cat}} \text{min g}_{\text{volatiles}}^{-1}$.

Catalyst deactivation is a problem for the scaling up of the process. However, the fluidized bed reactor is suitable to carry out the reforming step with catalyst circulation, with the catalyst being regenerated by coke combustion in another unit. In this case, the regenerated catalyst would partially contribute to providing the energy required in the reforming step.

Acknowledgement

This work was carried out with financial support from the Ministry of Economy and Competitiveness of the Spanish Government (CTQ2016-75535-R (AEI/FEDER, UE) and CTQ-2015-69436-R (MINECO/FEDER, UE)), the Basque Government (IT748-13) and the University of the Basque Country (UFI 11/39). I. Barbarias thanks the University of the Basque Country for her postgraduate grant (UPV/EHU 2016).

References

- [1] Ayalur Chattanathan S, Adhikari S, Abdoulmoumine N. A review on current status of hydrogen production from bio-oil. *Renew Sustain Energy Rev* 2012;16:2366–72.
- [2] Gollakota ARK, Reddy M, Subramanyam MD, Kishore N. A review on the upgradation techniques of pyrolysis oil. *Renew Sustain Energy Rev* 2016;58:1543–68.
- [3] Guan G, Kaewpanha M, Hao X, Abudula A. Catalytic steam reforming of biomass tar: prospects and challenges. *Renew Sustain Energy Rev* 2016;58:450–61.
- [4] Bridgwater AV. Review of fast pyrolysis of biomass and product upgrading. *Biomass Bioenergy* 2012;38:68–94.
- [5] Kan T, Strezov V, Evans TJ. Lignocellulosic biomass pyrolysis: a review of product properties and effects of pyrolysis parameters. *Renew Sustain Energy Rev* 2016;57:126–140.
- [6] Remiro A, Valle B, Aguayo AT, Bilbao J, Gayubo AG. Steam reforming of raw bio-oil in a fluidized bed reactor with prior separation of pyrolytic lignin. *Energy Fuels* 2013;27:7549–59.
- [7] Seyedejn-Azad F, Abedi J, Sampouri S. Catalytic steam reforming of aqueous phase of bio-oil over Ni-based alumina-supported catalysts. *Ind Eng Chem Res* 2014;53:17937–44.
- [8] Remón J, Broust F, Volle G, García L, Arauzo J. Hydrogen production from pine and poplar bio-oils by catalytic steam reforming. Influence of the bio-oil composition on the process. *Int J Hydrogen Energy* 2015;40:5593–608.
- [9] Czernik S, Evans R, French R. Hydrogen from biomass-production by steam reforming of biomass pyrolysis oil. *Catal Today* 2007;129:265–8.
- [10] Xu Q, Lan P, Zhang B, Ren Z, Yan Y. Hydrogen production via catalytic steam reforming of fast pyrolysis bio-oil in a fluidized-bed reactor. *Energy Fuels* 2010;24:6456–62.
- [11] Seyedejn Azad F, Abedi J, Salehi E, Harding T. Production of hydrogen via steam reforming of bio-oil over Ni-based catalysts: effect of support. *Chem Eng J* 2012;180:145–50.
- [12] Remiro A, Valle B, Aguayo AT, Bilbao J, Gayubo AG. Operating conditions for attenuating Ni/La₂O₃- α Al₂O₃ catalyst deactivation in the steam reforming of bio-oil aqueous fraction. *Fuel Process Technol* 2013;115:222–32.
- [13] Basagiannis AC, Verykios XE. Steam reforming of the aqueous fraction of bio-oil over structured Ru/MgO/Al₂O₃ catalysts. *Catal Today* 2007;127:256–64.
- [14] Kechagiopoulos PN, Voutetakis SS, Lemonidou AA, Vasalos IA. Hydrogen production via reforming of the aqueous phase of bio-oil over Ni/olivine catalysts in a spouted bed reactor. *Ind Eng Chem Res* 2009;48:1400–8.
- [15] Xiao X, Cao J, Meng X, et al. Synthesis gas production from catalytic gasification of waste biomass using nickel-loaded brown coal char. *Fuel* 2013;103:135–40.
- [16] Chen F, Wu C, Dong L, Vassallo A, Williams PT, Huang J. Characteristics and catalytic properties of Ni/CaAlO_x catalyst for hydrogen-enriched syngas production from pyrolysis-steam reforming of biomass sawdust. *Appl Catal B* 2016;183:168–75.
- [17] Arregi A, Lopez G, Amutio M, Barbarias I, Bilbao J, Olazar M. Hydrogen production from biomass by continuous fast pyrolysis and in-line steam reforming. *RSC Adv* 2016;6:25975–85.
- [18] Dong L, Wu C, Ling H, Shi J, Williams PT, Huang J. Promoting hydrogen production and minimizing catalyst deactivation from the pyrolysis-catalytic steam reforming of biomass on nanosized NiZnAlO_x catalysts. *Fuel* 2017;188:610–20.
- [19] Barbarias I, Lopez G, Alvarez J, et al. A sequential process for hydrogen production based on continuous HDPE fast pyrolysis and in-line steam reforming. *Chem Eng J* 2016;296:191–8.
- [20] Barbarias I, Lopez G, Arretxe M, et al. Pyrolysis and in-line catalytic steam reforming of polystyrene through a two-step reaction system. *J Anal Appl Pyrol* 2016;122:502–10.
- [21] Arregi A, Amutio M, Lopez G, et al. Hydrogen-rich gas production by continuous pyrolysis and in-line catalytic reforming of pine wood waste and HDPE mixtures. *Energy Convers Manage* 2017;136:192–201.
- [22] Erkiaga A, Lopez G, Amutio M, Bilbao J, Olazar M. Influence of operating conditions on the steam gasification of biomass in a conical spouted bed reactor. *Chem Eng J* 2014;237:259–67.
- [23] Alvarez J, Lopez G, Amutio M, Bilbao J, Olazar M. Upgrading the rice husk char obtained by flash pyrolysis for the production of amorphous silica and high quality activated carbon. *Bioresour Technol* 2014;170:132–7.
- [24] Amutio M, Lopez G, Alvarez J, Olazar M, Bilbao J. Fast pyrolysis of eucalyptus waste in a conical spouted bed reactor. *Bioresour Technol* 2015;194:225–32.
- [25] Erkiaga A, Lopez G, Barbarias I, et al. HDPE pyrolysis-steam reforming in a tandem spouted bed-fixed bed reactor for H₂ production. *J Anal Appl Pyrol* 2015;116:34–41.
- [26] Erika CE, Wu C, Williams PT. Syngas production from pyrolysis-catalytic steam reforming of waste biomass in a continuous screw kiln reactor. *J Anal Appl Pyrol* 2012;95:87–94.
- [27] Nahil MA, Wang X, Wu C, Yang H, Chen H, Williams PT. Novel bi-functional Ni-Mg-Al-CaO catalyst for catalytic gasification of biomass for hydrogen production with in situ CO₂ adsorption. *RSC Adv* 2013;3:5583–90.
- [28] Waheed QMK, Williams PT. Hydrogen production from high temperature pyrolysis/steam reforming of waste biomass: rice husk, sugar cane bagasse, and wheat straw. *Energy Fuels* 2013;27:6695–704.
- [29] Chen J, Sun J, Wang Y. Catalysts for steam reforming of bio-oil: a review. *Ind Eng Chem Res* 2017;56:4627–37.
- [30] Bartholomew CH. Mechanisms of catalyst deactivation. *Appl Catal A* 2001;212:17–60.
- [31] Li H, Xu Q, Xue H, Yan Y. Catalytic reforming of the aqueous phase derived from fast-pyrolysis of biomass. *Renew Energy* 2009;34:2872–7.

- [32] Hou T, Yuan L, Ye T, et al. Hydrogen production by low-temperature reforming of organic compounds in bio-oil over a CNT-promoting Ni catalyst. *Int J Hydrogen Energy* 2009;34:9095–107.
- [33] Zhang Y, Li W, Zhang S, Xu Q, Yan Y. Steam reforming of bio-oil for hydrogen production: effect of Ni-Co bimetallic catalysts. *Chem Eng Technol* 2012;35:302–8.
- [34] Rioche C, Kulkarni S, Meunier FC, Breen JP, Burch R. Steam reforming of model compounds and fast pyrolysis bio-oil on supported noble metal catalysts. *Appl Catal B* 2005;61:130–9.
- [35] Valle B, Remiro A, Aguayo AT, Bilbao J, Gayubo AG. Catalysts of Ni/ α -Al₂O₃ and Ni/La₂O₃- α -Al₂O₃ for hydrogen production by steam reforming of bio-oil aqueous fraction with pyrolytic lignin retention. *Int J Hydrogen Energy* 2013;38:1307–18.
- [36] Fu P, Yi W, Li Z, et al. Investigation on hydrogen production by catalytic steam reforming of maize stalk fast pyrolysis bio-oil. *Int J Hydrogen Energy* 2014;39:13962–71.
- [37] Lopez G, Erkiaga A, Artetxe M, Amutio M, Bilbao J, Olazar M. Hydrogen production by high density polyethylene steam gasification and in-line volatile reforming. *Ind Eng Chem Res* 2015;54:9536–44.
- [38] Alvarez J, Lopez G, Amutio M, Bilbao J, Olazar M. Bio-oil production from rice husk fast pyrolysis in a conical spouted bed reactor. *Fuel* 2014;128:162–9.
- [39] Elordi G, Olazar M, Lopez G, Artetxe M, Bilbao J. Continuous polyolefin cracking on an HZSM-5 zeolite catalyst in a conical spouted bed reactor. *Ind Eng Chem Res* 2011;50:6061–70.
- [40] Artetxe M, Lopez G, Amutio M, Elordi G, Bilbao J, Olazar M. Cracking of high density polyethylene pyrolysis waxes on HZSM-5 catalysts of different acidity. *Ind Eng Chem Res* 2013;52:10637–45.
- [41] Erkiaga A, Lopez G, Amutio M, Bilbao J, Olazar M. Syngas from steam gasification of polyethylene in a conical spouted bed reactor. *Fuel* 2013;109:461–9.
- [42] López G, Olazar M, Aguado R, Bilbao J. Continuous pyrolysis of waste tyres in a conical spouted bed reactor. *Fuel* 2010;89:1946–52.
- [43] Lopez G, Olazar M, Aguado R, et al. Vacuum pyrolysis of waste tires by continuously feeding into a conical spouted bed reactor. *Ind Eng Chem Res* 2010;49:8990–7.
- [44] Amutio M, Lopez G, Artetxe M, Elordi G, Olazar M, Bilbao J. Influence of temperature on biomass pyrolysis in a conical spouted bed reactor. *Resour Conserv Recycl* 2012;59:23–31.
- [45] Li D, Ishikawa C, Koike M, Wang L, Nakagawa Y, Tomishige K. Production of renewable hydrogen by steam reforming of tar from biomass pyrolysis over supported Co catalysts. *Int J Hydrogen Energy* 2013;38:3572–81.
- [46] Ma Z, Zhang S, Xie D, Yan Y. A novel integrated process for hydrogen production from biomass. *Int J Hydrogen Energy* 2014;39:1274–9.
- [47] Chen F, Wu C, Dong L, Jin F, Williams PT, Huang J. Catalytic steam reforming of volatiles released via pyrolysis of wood sawdust for hydrogen-rich gas production on Fe-Zn/Al₂O₃ nanocatalysts. *Fuel* 2015;158:999–1005.
- [48] Zou J, Yang H, Zeng Z, Wu C, Williams PT, Chen H. Hydrogen production from pyrolysis catalytic reforming of cellulose in the presence of K alkali metal. *Int J Hydrogen Energy* 2016;41:10598–607.
- [49] Xiao X, Meng X, Le DD, Takarada T. Two-stage steam gasification of waste biomass in fluidized bed at low temperature: parametric investigations and performance optimization. *Bioresour Technol* 2011;102:1975–81.
- [50] Wang Y, Hu X, Song Y, et al. Catalytic steam reforming of cellulose-derived compounds using a char-supported iron catalyst. *Fuel Process Technol* 2013;116:234–40.
- [51] Li D, Koike M, Chen J, Nakagawa Y, Tomishige K. Preparation of Ni-Cu/Mg/Al catalysts from hydrotalcite-like compounds for hydrogen production by steam reforming of biomass tar. *Int J Hydrogen Energy* 2014;39:10959–70.
- [52] Bimbela F, Oliva M, Ruiz J, García L, Arauzo J. Hydrogen production via catalytic steam reforming of the aqueous fraction of bio-oil using nickel-based coprecipitated catalysts. *Int J Hydrogen Energy* 2013;38:14476–87.
- [53] Liu S, Chen M, Chu L, et al. Catalytic steam reforming of bio-oil aqueous fraction for hydrogen production over Ni-Mo supported on modified sepiolite catalysts. *Int J Hydrogen Energy* 2013;38:3948–55.
- [54] Yao D, Wu C, Yang H, et al. Hydrogen production from catalytic reforming of the aqueous fraction of pyrolysis bio-oil with modified Ni-Al catalysts. *Int J Hydrogen Energy* 2014;39:14642–52.
- [55] Salehi E, Azad FS, Harding T, Abedi J. Production of hydrogen by steam reforming of bio-oil over Ni/Al₂O₃ catalysts: effect of addition of promoter and preparation procedure. *Fuel Process Technol* 2011;92:2203–10.
- [56] Seyedejn-Azad F, Salehi E, Abedi J, Harding T. Biomass to hydrogen via catalytic steam reforming of bio-oil over Ni-supported alumina catalysts. *Fuel Process Technol* 2011;92:563–9.
- [57] Czernik S, French R. Distributed production of hydrogen by auto-thermal reforming of fast pyrolysis bio-oil. *Int J Hydrogen Energy* 2014;39:744–50.
- [58] Yan C, Cheng F, Hu R. Hydrogen production from catalytic steam reforming of bio-oil aqueous fraction over Ni/CeO₂-ZrO₂ catalysts. *Int J Hydrogen Energy* 2010;35:11693–9.
- [59] Trimm DL. Coke formation and minimisation during steam reforming reactions. *Catal Today* 1997;37:233–8.
- [60] Angeli SD, Pilitsis FG, Lemonidou AA. Methane steam reforming at low temperature: Effect of light alkanes' presence on coke formation. *Catal Today* 2014;119–28.
- [61] Wu C, Williams PT. Investigation of coke formation on Ni-Mg-Al catalyst for hydrogen production from the catalytic steam pyrolysis-gasification of polypropylene. *Appl Catal B* 2010;96:198–207.
- [62] Blanco PH, Wu C, Williams PT. Influence of Ni/SiO₂ catalyst preparation methods on hydrogen production from the pyrolysis/reforming of refuse derived fuel. *Int J Hydrogen Energy* 2014;39:5723–32.
- [63] Barbarias I, Lopez G, Amutio M, et al. Steam reforming of plastic pyrolysis model hydrocarbons and catalyst deactivation. *Appl Catal A* 2016;527:152–60.
- [64] Sánchez-Sánchez MC, Navarro RM, Fierro JLG. Ethanol steam reforming over Ni/La-Al₂O₃ catalysts: influence of lanthanum loading. *Catal Today* 2007;129:336–45.
- [65] Zhang L, Li W, Liu J, Guo C, Wang Y, Zhang J. Ethanol steam reforming reactions over Al₂O₃/SiO₂-supported Ni-La catalysts. *Fuel* 2009;88:511–8.
- [66] He Z, Yang M, Wang X, Zhao Z, Duan A. Effect of the transition metal oxide supports on hydrogen production from bio-ethanol reforming. *Catal Today* 2012;194:2–8.
- [67] Lin K, Wang C, Chien S. Catalytic performance of steam reforming of ethanol at low temperature over LaNiO₃ perovskite. *Int J Hydrogen Energy* 2013;38:3226–32.
- [68] Vicente J, Montero C, Ereña J, Azkoiti MJ, Bilbao J, Gayubo AG. Coke deactivation of Ni and Co catalysts in ethanol steam reforming at mild temperatures in a fluidized bed reactor. *Int J Hydrogen Energy* 2014;39:12586–96.
- [69] Montero C, Ochoa A, Castaño P, Bilbao J, Gayubo AG. Monitoring Ni⁰ and coke evolution during the deactivation of a Ni/La₂O₃- α -Al₂O₃ catalyst in ethanol steam reforming in a fluidized bed. *J Catal* 2015;331:181–92.
- [70] Vicente J, Ereña J, Montero C, Azkoiti MJ, Bilbao J, Gayubo AG. Reaction pathway for ethanol steam reforming on a Ni/SiO₂ catalyst including coke formation. *Int J Hydrogen Energy* 2014;39:18820–34.
- [71] Wang Z, Pan Y, Dong T, et al. Production of hydrogen from catalytic steam reforming of bio-oil using C12A7-O-based catalysts. *Appl Catal A* 2007;320:24–34.
- [72] Wu C, Huang Q, Sui M, Yan Y, Wang F. Hydrogen production via catalytic steam reforming of fast pyrolysis bio-oil in a two-stage fixed bed reactor system. *Fuel Process Technol* 2008;89:1306–16.
- [73] Lan P, Xu Q, Zhou M, Lan L, Zhang S, Yan Y. Catalytic steam reforming of fast pyrolysis bio-oil in fixed bed and fluidized bed reactors. *Chem Eng Technol* 2010;33:2021–8.
- [74] Cao J, Shi P, Zhao X, Wei X, Takarada T. Catalytic reforming of volatiles and nitrogen compounds from sewage sludge pyrolysis to clean hydrogen and synthetic gas over a nickel catalyst. *Fuel Process Technol* 2014;123:34–40.
- [75] Shen Y, Chen M, Sun T, Jia J. Catalytic reforming of pyrolysis tar over metallic nickel nanoparticles embedded in pyrochar. *Fuel* 2015;159:570–9.
- [76] Garcia L, French R, Czernik S, Chornet E. Catalytic steam reforming of bio-oils for the production of hydrogen: effects of catalyst composition. *Appl Catal A* 2000;201:225–39.
- [77] Lan P, Lan LH, Xie T, Liao AP. The preparation of syngas by the reforming of bio-oil in a fluidized-bed reactor. *Energy Sources Part A* 2014;36:242–9.
- [78] Xie H, Yu Q, Zuo Z, Han Z, Yao X, Qin Q. Hydrogen production via sorption-enhanced catalytic steam reforming of bio-oil. *Int J Hydrogen Energy* 2016;41:2345–53.
- [79] Medrano JA, Oliva M, Ruiz J, García L, Arauzo J. Hydrogen from aqueous fraction of biomass pyrolysis liquids by catalytic steam reforming in fluidized bed. *Energy* 2011;36:2215–24.
- [80] Czernik S, French R, Feik C, Chornet E. Hydrogen by catalytic steam reforming of liquid byproducts from biomass thermoconversion processes. *Ind Eng Chem Res* 2002;41:4209–15.
- [81] Joensen F, Rostrup-Nielsen JR. Conversion of hydrocarbons and alcohols for fuel cells. *J Power Sources* 2002;105:195–201.